

Phase-Only Control of Peak Sidelobe Level and Pattern Nulls Using Iterative Phase Perturbations

Aslan, Yanki; Puskely, Jan; Roederer, Antoine; Yarovoy, Alexander

DOI

[10.1109/LAWP.2019.2937682](https://doi.org/10.1109/LAWP.2019.2937682)

Publication date

2019

Document Version

Final published version

Published in

IEEE Antennas and Wireless Propagation Letters

Citation (APA)

Aslan, Y., Puskely, J., Roederer, A., & Yarovoy, A. (2019). Phase-Only Control of Peak Sidelobe Level and Pattern Nulls Using Iterative Phase Perturbations. *IEEE Antennas and Wireless Propagation Letters*, 18(10), 2081-2085. [8818285]. <https://doi.org/10.1109/LAWP.2019.2937682>

Important note

To cite this publication, please use the final published version (if applicable). Please check the document version above.

Copyright

Other than for strictly personal use, it is not permitted to download, forward or distribute the text or part of it, without the consent of the author(s) and/or copyright holder(s), unless the work is under an open content license such as Creative Commons.

Takedown policy

Please contact us and provide details if you believe this document breaches copyrights. We will remove access to the work immediately and investigate your claim.


Green Open Access added to TU Delft Institutional Repository

'You share, we take care!' – Taverne project

<https://www.openaccess.nl/en/you-share-we-take-care>

Otherwise as indicated in the copyright section: the publisher is the copyright holder of this work and the author uses the Dutch legislation to make this work public.

Phase-Only Control of Peak Sidelobe Level and Pattern Nulls Using Iterative Phase Perturbations

Yanki Aslan , *Graduate Student Member, IEEE*, Jan Puskely, Antoine Roederer, *Life Fellow, IEEE*, and Alexander Yarovoy, *Fellow, IEEE*

Abstract—Minimization of the maximum sidelobe level for a given array geometry, amplitude distribution, and nulling sectors by phase-only adjustment of the element coefficients is studied. Nonlinear optimization problem for phase distribution is solved using a novel iterative convex optimization algorithm, which includes mutual coupling effects and exploits small phase perturbations at each step. Superiority of the algorithm in terms of the peak sidelobe level and nulling depth achieved over several optimization methods reported in the most relevant literature is demonstrated in several case studies. Finally, a case study is performed to demonstrate added value of the algorithm for millimeter-wave fifth generation application with phase-only radiation pattern forming.

Index Terms—Convex optimization, fifth generation (5G), interference minimization, null steering, phased arrays, phase-only control, phase tapering.

I. INTRODUCTION

THE future fifth generation (5G) antenna systems are expected to serve multiple users simultaneously in the same frequency band using a single multibeam array with space-division multiple access (SDMA) [1]. Since such systems are dominated by the interference rather than the noise, suppressing the interuser interferences is very crucial for higher communication quality and capacity [2].

In array synthesis with given element locations, interference suppression by controlling the complex excitation weights (amplitudes, phases) at each antenna element provides the most degrees of freedom and best pattern performances. However, it is also the most expensive strategy due to the need of both a phase shifter and a variable gain amplifier (or attenuator) per element. Considering this drawback, phase-only tapering has been introduced, which exploits the phase shifters used for beam steering in phased arrays also to obtain low sidelobes and nulls, while maintaining a relatively simpler feed network and higher power efficiency as compared with the amplitude-tapered arrays [3]. Such an approach is more attractive for the 5G market in which system cost is of extreme importance.

Manuscript received August 5, 2019; revised August 23, 2019; accepted August 23, 2019. Date of publication August 28, 2019; date of current version October 4, 2019. This work was supported in part by NWO and in part by NXP Semiconductors in the framework of the partnership program on Advanced 5G Solutions within the Project 15590 titled “Antenna Topologies and Front-end Configurations for Multiple Beam Generation.” (*Corresponding author: Yanki Aslan.*)

The authors are with the Department of Microelectronics, Microwave Sensing, Signals and Systems Group, Delft University of Technology, Delft 2600, The Netherlands (e-mail: Y.Aslan@tudelft.nl; J.Puskely-1@tudelft.nl; A.G.Roederer@tudelft.nl; A.Yarovoy@tudelft.nl).

Digital Object Identifier 10.1109/LAWP.2019.2937682

Being inherently nonlinear, phase-only pattern design problem has been studied in the literature by employing a large variety of synthesis strategies. Phase-only pattern shaping with a prespecified mask was studied using deterministic methods [4], numerical approaches [5], [6], and population-based optimization techniques like genetic algorithm [7]. In [8], best common amplitude distribution was searched for several beam shapes (flat-topped, cosecant, and pencil) in reconfigurable arrays with phase-only control using the intersection approach. The same problem was addressed in [9] and [10] using convex optimization and in [11] using vector projection approach.

Considering multiuser communication aspects, statistical interference suppression via peak sidelobe level (SLL) minimization [12] with phase-only tapering was also studied using steepest descent method [3], iterative fast Fourier transform [13], and iterative projection method [14]. Furthermore, it was shown that phase tapering is effective in pattern nulling of both narrow [15] and wide [16] angular sectors. Recently, in [17], a phase-only method based on successive alternating projections was used in uniform-amplitude arrays to create Gaussian-shaped null regions for 5G applications.

In this letter, we propose a novel phase-only, mutual coupling (MC) aware peak SLL minimization and (simultaneous) pattern nulling technique that is based on iterative convex optimization. The nonlinear problem is linearized by introducing small phase perturbations at each iteration. The algorithm performance is compared with several techniques reported in the literature, and its superiority is shown by examples. Finally, a case study is performed to demonstrate added value of the algorithm for millimeter (mm)-wave 5G application with phase-only radiation pattern forming. The rest of this letter is organized as follows. Section II presents the formulation of the optimization steps. Section III shows the comparative simulation results. The conclusions are given in Section IV.

II. FORMULATION OF THE OPTIMIZATION PROBLEM

For an array with configuration given in Fig. 1, the far field $f^{i,s}$ at the i th iteration of the algorithm for a scanned beam s is given by

$$f^{i,s}(\theta, \phi) = \sum_{n=1}^N f_n(\theta, \phi) w_n^{i,s} e^{jk_0(x_n \sin \theta \cos \phi + y_n \sin \theta \sin \phi)} \quad (1)$$

where f_n is the complex far-field of the n th element when the field origin is at the element center, k_0 is the wavenumber, (x_n, y_n) denotes the position of the n th element, and $w_n^{i,s}$ is the excitation weight of the n th element at the i th iteration for a

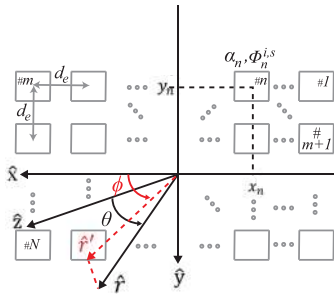


Fig. 1. Schematic of a uniform planar array of N patch antennas. θ is the elevation angle defined as the angle between the observation direction \hat{r} and \hat{z} . The unit vector \hat{r}' is the projection of \hat{r} onto the $\hat{x}\hat{y}$ plane. ϕ is the azimuth angle defined as the angle between \hat{r}' and \hat{x} .

scanned beam s . The excitation weights are given by

$$w_n^{i,s} = \alpha_n e^{j(\Phi_n^{i-1,s} + \Phi_n^{i,s})} \quad (2)$$

where α_n is the pre-given amplitude and $\Phi_n^{i,s}$ is the phase variation of the n th element at the i th iteration (with respect to the element phase at the previous iteration) for a scanned beam s .

Let us introduce the u - v coordinates as follows:

$$\begin{aligned} u &= \sin \theta \cos \phi, & u_s &= \sin \theta_s \cos \phi_s \\ v &= \sin \theta \sin \phi, & v_s &= \sin \theta_s \sin \phi_s \end{aligned} \quad (3)$$

where θ_s, ϕ_s (and the corresponding u_s, v_s) represent the desired beam pointing direction for a scanned beam s .

Assuming $|\Phi_n^{i,s}| \ll 1$, and using the first-order Taylor expansion, (1) can be approximated and written as follows:

$$f^{i,s}(u, v) = \sum_{n=1}^N f_n(u, v) \alpha_n e^{j\Phi_n^{i-1,s}} (1 + j\Phi_n^{i,s}) e^{jk_0(x_n u + y_n v)}. \quad (4)$$

The initial phases for the beam s are given by

$$\Phi_n^{0,s} = -k_0(x_n u_s + y_n v_s). \quad (5)$$

Overall, the optimization problem at the i th iteration of the algorithm becomes

$$\min_{\Phi^{i,s}} \rho^i, \quad \text{s.t.} \quad \begin{cases} |f^{i,s}(\{\mathbf{u}, \mathbf{v}\}_{SL,s})| \leq \rho^i \\ f^{i,s}(u_s, v_s) = 1 \\ |f^{i,s}(\{\mathbf{u}, \mathbf{v}\}_{NR,s})| \leq \delta \\ |\Phi_n^{i,s}| \leq \mu, \quad \forall n \in \{1, 2, \dots, N\} \end{cases} \quad (6)$$

where $\{\mathbf{u}, \mathbf{v}\}_{SL,s}$ and $\{\mathbf{u}, \mathbf{v}\}_{NR,s}$ define the sidelobe and null regions, respectively. ρ^i is the maximum SLL to be minimized at the i th iteration. δ is the suppression level in the null region. μ defines the upper bound of the phase perturbations such that $|\Phi_n^{i,s}| \ll 1$, which is needed to properly apply the Taylor expansion in (4).

The optimization problem presented in (6) is a second-order cone program (SOCP) problem where a linear function is minimized over the intersection of an affine set and the product of quadratic cones [18]. For a comprehensive introduction to SOCP and its applications, the interested readers are referred

to [18] and [19]. Many approaches exist in the literature to efficiently solve the SOCP problems. Some examples include interior-point method (IPM) [18], [20], reduced-augmented-equation approach [21], pivoting method [22], and parametric approach [23]. Today, SOCP problems can be easily solved in polynomial time by available convex programming toolboxes [24], [25] using IPM, which is commonly exploited by antenna researchers [26]–[29]. In this letter, CVX, a MATLAB-based modeling system for convex optimization, is used to formulate and solve the problem in (6).

III. SYNTHESIS RESULTS

In this section, the proposed algorithm's performance is evaluated by comparative case studies presented in the related literature with additional realistic, MC embedded patterns and 5G-oriented examples. In the simulations, it is assumed that $\mu = \pi/3$ and $\delta = 0.0001$. All numerical computations have been carried out on an Intel Core i7-4710HQ 2.5 GHz CPU, 16 GB RAM computer. Each iteration takes about a few seconds in the linear arrays and an hour in the considered 64-element planar array for a uniform discretization step of 0.01 in the u - v plane. It is also worthy to note that, in this letter, we do not adopt a stop condition. Instead, we define a maximum number of iterations and observe the behavior of the maximum SLL to study its convergence. However, such a condition can be specified considering the relative change in the peak SLL in a few successive iterations so that the iterative process stops when the maximum SLL no longer diminishes. An example is to stop when $20 \log(\rho^i / \rho^{i-1}) \leq 0.01$, as applied in [28]. If there is a peak SLL targeted for a system, it is also possible to stop the iterations as soon as the aim is reached.

Case-1: First, the results of the presented convex optimization method are compared with the phase-only synthesis technique presented in [3]. Using the steepest descent method, DeFord and Gandhi [3] tried to minimize the peak SLL, which is the same goal function that is used in this letter. As done in [3], the synthesis is performed on the array factor (AF) where α_n is the same for all n and the phases are even-symmetric. Note that the even-symmetry can be easily enforced using an additional constraint, $\Phi_n^{i,s} = \Phi_{N-n+1}^{i,s}$ for even N , in (6). The interelement spacing d_e is equal to $0.5\lambda_0$. The maximum iteration number is set to 20. The comparison is given in terms of the maximum SLL, first-null beamwidth (FNBW), half-power beamwidth (HPBW), and array efficiency (which is defined as the ratio of the peak power density of the phase (and/or amplitude) tapered array to the peak power density of the uniformly excited array with progressive phase shifts defined by the scan angle). Table I provides a summary of the results for the linear array with $N = 20, 40$, and 80. It can be seen that the convex optimization provides competitive or better (especially for the relatively smaller array with $N = 20$) results. The synthesized array pattern, element phases, and maximum SLL convergence for $N = 40$ with the presented method are also given in Fig. 2 for comparison with Case-2, which is studied next.

Case-2: The AF-only optimization in Case-1 does not consider the MC effects and may result in unreliable patterns. In Case-2, full-wave simulations are performed using a conventional pin-fed patch antenna in a 40-element $\lambda_0/2$ spaced E -plane array at a candidate 5G frequency of 28 GHz. Upon using equiamplitude element excitations, due to the difference

TABLE I
PERFORMANCE COMPARISON BETWEEN THE STEEPEST DESCENT METHOD IN [3] AND THIS METHOD IN THE CASE OF PHASE-ONLY ARRAY SYNTHESIS WITH UNIFORM AMPLITUDES

Number of elements (N)	Steepest Descent Method in [3]			This method		
	Peak SLL (dB)	FNBW (deg.)	Eff. (%)	Peak SLL (dB)	FNBW (deg.)	Eff. (%)
20	-15.8	12.5	81.8	-16.1	12.2	83.6
40	-17.9	6.3	76.6	-18.1	6.4	74.7
80	-20.1	3.4	69.6	-20.3	3.4	67.3

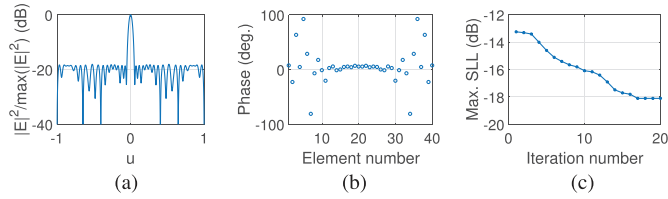


Fig. 2. Results of Case-1 for $N = 40$. (a) Normalized AF (at iteration number 20). (b) Even-symmetric element phases (at iteration number 20). (c) Iterative trend of the maximum SLL.

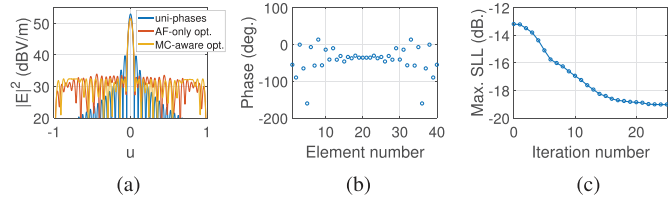


Fig. 3. Results of Case-2 for $N = 40$. (a) Far E -field pattern (at iteration number 25). (b) Even-symmetric element phases (at iteration number 25). (c) Iterative trend of the maximum SLL.

in the embedded patterns, the AF-only optimized phases lead to a modified final pattern [compare Fig. 3(a) with Fig. 2(a)], a maximum SLL of -17.7 instead of -18.1 dB, and an efficiency of 74.1% instead of 74.7% as reported in Table I. By inserting the embedded patterns in the presented MC-aware method, we are able to synthesize a reliable pattern with a maximum SLL of -19.0 dB, but with an efficiency of 70.6% . The maximum iteration number is now set to 25. The E -field pattern, even-symmetric element phases, and convergence results of the MC-aware optimization with a 40-element E -plane patch array are shown in Fig. 3.

Case-3: In this part, the aim is to compute the phases of the array elements for a fixed subarray amplitude weighting in order to minimize the maximum SLL, as studied in [14]. The N -element array is partitioned into Q uniform and contiguous subarrays with a Taylor taper. Two cases are studied here for direct comparison with the results in [14]: 1) $N = 128$, $Q = 8$; and 2) $N = 32$, $Q = 4$. It is assumed that the elements are isotropic and separated uniformly by $\lambda_0/2$. The phases are forced to be even-symmetric. For completeness, the AFs, element amplitudes, and phases for $(N, Q) = (128, 8)$ and $(N, Q) = (32, 4)$ are given in Figs. 4 and 5, respectively. A comparison with the iterative projection method in [14] is provided in Table II. It can be seen that the presented technique outperforms it in terms of

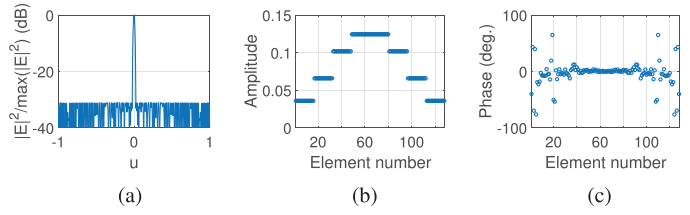


Fig. 4. Results of Case-3 for $N = 128$, $Q = 8$. (a) Normalized AF. (b) Even-symmetric element amplitudes. (c) Even-symmetric element phases.

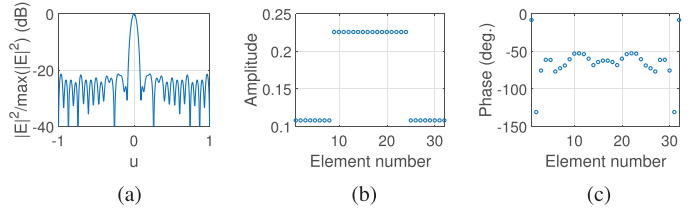


Fig. 5. Results of Case-3 for $N = 32$, $Q = 4$. (a) Normalized AF. (b) Even-symmetric element amplitudes. (c) Even-symmetric element phases.

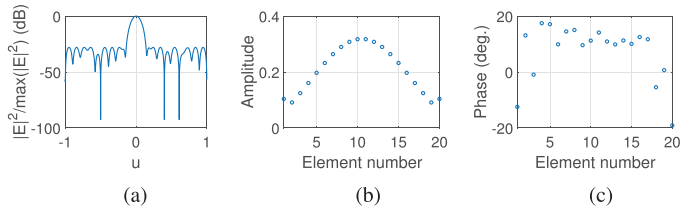


Fig. 6. Results of Case-4 for $N = 20$ with phase-only control. (a) Normalized AF. (b) Element amplitudes. (c) Element phases.

the maximum SLL and efficiency in the case of the large array with $N = 128$ elements. For the smaller array, the efficiency is 3.7% larger, whereas the maximum SLL increases by 0.3 dB.

Case-4: Many pattern control methods in the literature study pattern nulling with prespecified amplitude tapering for SLL reduction and phase perturbation for creating the zeros. Here, we focus on pattern nulling by phase control for narrow-sector interferers as studied in [15]. For fair comparison, we consider $N = 20$ isotropic elements with $0.5\lambda_0$ regular spacing. Three nulls are placed at $u = \{-0.5, 0.4, 0.61\}$. In [15], the Levenberg–Marquardt algorithm was used by targeting the array pattern as the envelope of the 30 dB Dolph–Chebyshev amplitude taper. At the output, -80 dB null levels were obtained with a maximum SLL of -25 dB. First, we assume a 30 dB Chebyshev windowing and optimize the phases to minimize the maximum SLL while nulling out the interferences. The results in this case are summarized in Fig. 6. It is seen that using the proposed method, the null levels become -92 dB and the maximum SLL is reduced to -28 dB. Second, we consider a phase-only tapering with equiamplitude element excitations for the same array topology and optimization goal, which is more preferable for reduced design complexity and increased efficiency. For the uniform-amplitude counterpart, similar to the Chebyshev tapered array, -92 dB nulls are observed. However, the maximum SLL becomes -15.6 dB.

Case-5: The problem of broad-sector nulling and simultaneous SLL minimization is considered in this part. The proposed

TABLE II
PERFORMANCE COMPARISON BETWEEN THE ITERATIVE PROJECTION METHOD IN [14] AND THIS METHOD IN THE CASE OF UNIFORM SUBARRAYED ARRAY ANTENNAS

Number of elements (N)	Number of sub-arrays (Q)	No phase taper			Iterative projection method in [14]			This method		
		Peak SLL (dB)	HPBW (deg.)	Eff. (%)	Peak SLL (dB)	HPBW (deg.)	Eff. (%)	Peak SLL (dB)	HPBW (deg.)	Eff. (%)
128	8	-25.1	1.0	84.3	-29.2	1.1	78.5	-31.1	1.1	79.2
32	4	-18.6	3.9	86.3	-21.7	4.2	76.6	-21.4	4.0	80.3

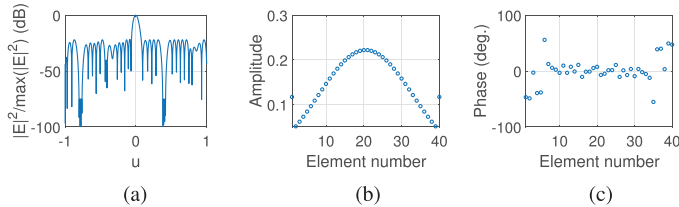


Fig. 7. Results of Case-5 for $N = 40$ with phase-only control. (a) Normalized AF. (b) Element amplitudes. (c) Odd-symmetric element phases.

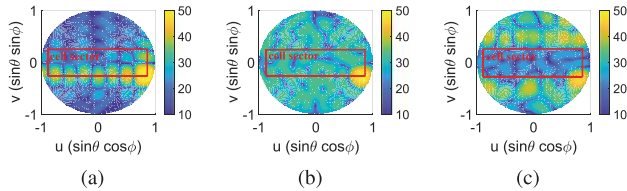


Fig. 8. Far E -field patterns (in dBV/m) of the 8×8 patch array in Case-6 for a beam scanned toward the 5G cell sector edge $u_s = \sin(\pi/3)$, $v_s = -\sin(\pi/12)$ for (a) progressive phases, (b) phases optimized for minimum SLL everywhere in the visible region, and (c) phases optimized for minimum SLL in the sector.

algorithm's performance is illustrated using the numerical example in [16] with $N = 40$ isotropic, $\lambda_0/2$ spaced elements. Two sector nulls at $u = [-0.8 \ -0.76]$ and $u = [0.38 \ 0.42]$ are desired. The phases are assumed to be odd-symmetric to reduce the number of calculations as done in [16]. Using a 30 dB Chebyshev initial amplitude taper, sector depths around -70 and -80 dB were obtained in the linear programming technique in [16] while having a maximum SLL around -19 dB. For the same initial settings, our method provides sector depths of -75 dB while keeping the maximum SLL at -22 dB. The results for this case are summarized in Fig. 7. For phase-only tapering with a uniform amplitude array, our method is able to decrease the maximum SLL to -16.2 dB while keeping the sector nulls at -75 dB.

Case-6: In the last case, we study SLL minimization for an 8×8 $\lambda_0/2$ spaced uniform-amplitude patch antenna array at 28 GHz considering a typical 5G angular cell sector ($\pm 15^\circ$ in elevation and $\pm 60^\circ$ in azimuth) [30] and using our phase-only tapering algorithm. The embedded far-field pattern of each patch element is computed to include the impact of MC. The beam is steered toward the cell edge, i.e., $u_s = \sin(\pi/3)$, $v_s = -\sin(\pi/12)$. The maximum iteration number is set to 25. Fig. 8(a) shows the pattern for the standard progressive phase shifts, for which the maximum SLL is -9.1 dB. For SLL minimization everywhere in the visible region, the pattern in Fig. 8(b) and the phases in Fig. 9(a) are observed with a maximum SLL of -15.7 dB

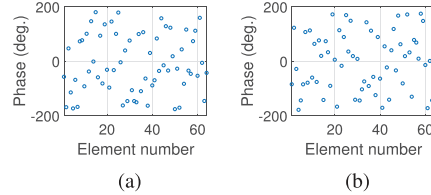


Fig. 9. Element phases at iteration number 25 with $\mu = \pi/3$ in Case-6 with optimization for minimum SLL (a) everywhere in the visible region and (b) in the sector.

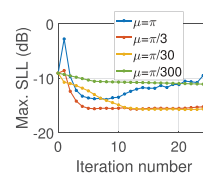


Fig. 10. Maximum SLL trend with μ for optimization everywhere in the visible region.

and efficiency of 55%. For completeness, the convergence of the maximum SLL for varying μ values is plotted in Fig. 10. It can be seen that the chosen value of $\mu = \pi/3$ provides a stable convergence within a reasonable number of iterations ($= 5$). If the optimization is done to minimize the interference in the sector, the pattern in Fig. 8(c) is obtained with the phases given in Fig. 9(b). In this case, the maximum SLL in the sector becomes as low as -18.5 dB, but the efficiency drops to 30%.

IV. CONCLUSION

This letter presents a new phase-only peak SLL minimization and simultaneous pattern nulling algorithm. The nonlinear optimization problem is linearized using an iterative procedure by introducing small phase perturbations on the element excitation coefficients at each iteration. Embedded element patterns, which are obtained via full-wave simulations, can be integrated into the optimization procedure. In terms of the peak SLL reduction, the proposed approach outperforms the existing methods when radiation pattern nulling in certain sectors is required and achieves at least comparative results in cases without nulling, as illustrated via the case studies. The proposed phase-only radiation pattern control method is promising for the initial, low-cost 5G base station antennas serving multiple SDMA users at millimeter waves.

ACKNOWLEDGMENT

The authors would like to thank Dr. P. Angeletti for the useful discussion that initiated this letter.

REFERENCES

- [1] Y. Aslan, J. Puskely, J. H. J. Janssen, M. Geurts, A. Roederer, and A. Yarovoy, "Thermal-aware synthesis of 5G base station antenna arrays: An overview and a sparsity-based approach," *IEEE Access*, vol. 6, pp. 58868–58882, 2018.
- [2] Y. Aslan, S. Salman, J. Puskely, A. Roederer, and A. Yarovoy, "5G multi-user system simulations in line-of-sight with space-tapered cellular base station phased arrays," in *Proc. 13th Eur. Conf. Antennas Propag.*, Krakow, Poland, Apr. 2019, pp. 1–5.
- [3] J. F. DeFord and O. P. Gandhi, "Phase-only synthesis of minimum peak sidelobe patterns for linear and planar arrays," *IEEE Trans. Antennas Propag.*, vol. 36, no. 2, pp. 191–201, Feb. 1988.
- [4] A. F. Morabito, T. Isernia, and L. D. Donato, "Optimal synthesis of phase-only reconfigurable linear sparse arrays having uniform-amplitude excitations," *Prog. Electromagn. Res.*, vol. 124, pp. 405–423, 2012.
- [5] E. Ercil, "An alternative method for phase only array pattern synthesis," in *Proc. IEEE Int. Symp. Antennas Propag.*, Chicago, IL, USA, Jul. 2012, pp. 1–2.
- [6] J. Liang, X. Fan, W. Fan, D. Zhou, and J. Li, "Phase-only pattern synthesis for linear antenna arrays," *IEEE Antennas Wireless Propag. Lett.*, vol. 16, pp. 3232–3235, 2017.
- [7] D. W. Boeringer and D. H. Werner, "Adaptive mutation parameter toggling genetic algorithm for phase-only array synthesis," *Electron. Lett.*, vol. 38, no. 25, pp. 1618–1619, Dec. 2002.
- [8] O. Bucci, G. Mazzarella, and G. Panariello, "Reconfigurable arrays by phase-only control," *IEEE Trans. Antennas Propag.*, vol. 39, no. 7, pp. 919–925, Jul. 1991.
- [9] B. Fuchs, "Application of convex relaxation to array synthesis problems," *IEEE Trans. Antennas Propag.*, vol. 62, no. 2, pp. 634–640, Feb. 2014.
- [10] P. J. Kajenski, "Phase only antenna pattern notching via a semidefinite programming relaxation," *IEEE Trans. Antennas Propag.*, vol. 60, no. 5, pp. 2562–2565, May 2012.
- [11] G. Buttazzoni and R. Vescovo, "Reconfigurable antenna arrays with phase-only control in the presence of near-field nulls," *J. Inf. Commun. Technol.*, vol. 3, pp. 88–93, Jan. 2017.
- [12] Y. Aslan, J. Puskely, A. Roederer, and A. Yarovoy, "Trade-offs between the quality of service, computational cost and cooling complexity in interference-dominated multi-user SDMA systems," *IET Commun.*, to be published.
- [13] P. Harikumar, V. B. Bikkani, G. Mahanti, and B. Mahato, "Phase-only side lobe level reduction of uniformly excited linear array antenna using iterative fast Fourier transform," in *Proc. IEEE India Conf.*, Hyderabad, India, Dec. 2011, pp. 1–4.
- [14] P. Rocca, R. L. Haupt, and A. Massa, "Sidelobe reduction through element phase control in uniform subarrayed array antennas," *IEEE Antennas Wireless Propag. Lett.*, vol. 8, pp. 437–440, 2009.
- [15] T. H. Ismail, D. I. Abu-Al-Nadi, and M. J. Mismar, "Phase-only control for antenna pattern synthesis of linear arrays using the Levenberg-Marquardt algorithm," *Electromagnetics*, vol. 24, no. 7, pp. 555–564, Jun. 2010.
- [16] M. J. Mismar and T. H. Ismail, "Pattern nulling by iterative phase perturbation," *Prog. Electromagn. Res.*, vol. 22, pp. 181–195, 1999.
- [17] G. Buttazzoni, M. Comisso, F. Ruzzier, and R. Vescovo, "Phase-only antenna array reconfigurability with Gaussian-shaped nulls for 5G applications," *Int. J. Antennas Propag.*, vol. 2019, Feb. 2019, Art. no. 9120530.
- [18] M. Lobo, L. Vandenberghe, S. Boyd, and H. Lebert, "Applications of second-order cone programming," *Linear Algebra Its Appl.*, vol. 284, no. 1–3, pp. 193–228, 1998.
- [19] F. Alizadeh and D. Goldfarb, "Second-order cone programming," *Math. Program.*, vol. 95, no. 1, pp. 3–51, 2003.
- [20] Y.-J. Kuo and H. Mittelmann, "Interior point methods for second-order cone programming and OR applications," *Comput. Optim. Appl.*, vol. 28, no. 3, pp. 255–285, 2004.
- [21] Z. Cai and K. Toh, "Solving second order cone programming via a reduced augmented system approach," *SIAM J. Optim.*, vol. 17, no. 3, pp. 711–737, 2006.
- [22] M. Muramatsu, "A pivoting procedure for a class of second-order cone programming," *Optim. Methods Softw.*, vol. 21, pp. 295–314, 2006.
- [23] T. Hasuike, "On an exact optimal solution for a second-order cone programming problem," in *Proc. Int. MultiConf. Engineers Comput. Scientists*, Hong Kong, Mar. 2011, pp. 1484–1488.
- [24] M. Grant and S. Boyd, "CVX: Matlab software for disciplined convex programming, version 2.1," Mar. 2014. [Online]. Available: <http://cvxr.com/cvx>
- [25] J. F. Sturm, "Using SeDuMi 1.02, a MATLAB toolbox for optimization over symmetric cones," *Optim. Methods Softw.*, vol. 11–12, pp. 625–653, 1999.
- [26] H. B. Van, S. N. Jha, and C. Craeye, "Fast full-wave synthesis of printed antenna arrays including mutual coupling," *IEEE Trans. Antennas Propag.*, vol. 64, no. 12, pp. 5163–5171, Dec. 2016.
- [27] S. E. Nai, W. Ser, Z. L. Yu, and H. Chen, "Beampattern synthesis for linear and planar arrays with antenna selection by convex optimization," *IEEE Trans. Antennas Propag.*, vol. 58, no. 12, pp. 3923–3930, Dec. 2010.
- [28] B. Fuchs, A. Skrivervik, and J. R. Mosig, "Synthesis of uniform amplitude focused beam arrays," *IEEE Antennas Wireless Propag. Lett.*, vol. 11, pp. 1178–1181, 2012.
- [29] M. D'Urso, G. Prisco, and R. M. Tumolo, "Maximally sparse, steerable, and nonsuperdirective array antennas via convex optimizations," *IEEE Trans. Antennas Propag.*, vol. 64, no. 9, pp. 3840–3849, Sep. 2016.
- [30] E. Degirmenci, "EMF test report: Ericsson AIR 5121," Ericsson AB, Stockholm, Sweden, Tech. Rep. GFTB-17:001589 Uen Rev B, Jan. 2018.